

RESEARCH ARTICLE

Open Access

New Zealand Journal of Forestry Science

Long term monitoring of red needle cast: what drives episodic outbreaks on radiata pine in New Zealand?

Stuart Fraser*†, Emily McLay, Christine Todoroki, Nicolò Camarretta and Ian Hood‡

Scion Group, New Zealand Institute for Bioeconomy Science, Private Bag 3020, Rotorua 3046, New Zealand

*Corresponding author: stuart.fraser@scionresearch.com

† Authors with equal contribution

(Received for publication 26 March 2025; accepted in revised form 22 June 2025)

Editor: Horacio E. Bown

Abstract

Background: Red needle cast (RNC) is a foliar disease of radiata pine (*Pinus radiata* D.Don) in New Zealand caused by *Phytophthora pluvialis* Reeser, W.L.Sutton & E.M.Hansen and, to a lesser extent, *Phytophthora kernoviae* Brasier, Beales & S.A.Kirk. Incidence and severity of RNC vary substantially between years. To investigate the impact of seasonal weather variables on this variation, RNC was assessed annually for ten years at radiata pine transects.

Methods: Fifty-three transects were established in 2015 in the Central North Island and Gisborne Region (east coast North Island) of New Zealand, with twenty-three monitored until 2024 (surviving harvest). The relationship between seasonal weather variables and RNC severity was analysed using two non-parametric statistical approaches: (1) correlation analyses (Spearman correlations, r_s , where positive values indicate an increase in RNC severity with an increase in the explanatory variable); and (2) binary recursive partitioning (with models trained on 85% of observations and tested on the remaining 15%).

Results: Disease expressed more consistently, and severity was generally greater, at Gisborne sites. Disease severity peaked in 2017 and 2023 in both regions. Autumn (March-May) variables tended to be prevalent amongst predictors of RNC severity. Autumn soil moisture index (calculated from cumulative rainfall and evapotranspiration) was the most strongly correlated variable for the Gisborne dataset ($r_s = 0.70$) and, along with vapour pressure, were the key partitioning variables in the recursive partitioning model. The strongest correlating variable for the Central North Island dataset was autumn potential evapotranspiration ($r_s = -0.46$) while the most important variable and first data partition was autumn vapour pressure. Model evaluation metrics indicated good performance: R^2 values were 0.63 and 0.68 for the Gisborne and Central North Island test datasets respectively, and mean absolute errors were 18.1 % and 7.8 % for the respective datasets.

Conclusions: The importance of autumn more than summer weather variables in determining disease expression differs from the findings of previous studies and indicates that conditions during periods of exponential epidemic growth may be as, or more, important than initial inoculum level in determining RNC severity. Proactive control activities may require long-term weather forecasting or frequent monitoring during this season.

Keywords: Climatic variables, foliar disease, forest disease, needle disease, polycyclic disease epidemiology, weather variables

Introduction

The frequency and severity of plant disease epidemics are strongly influenced by environmental factors, such as temperature and precipitation. Within a year, weather regulates the behaviour of pathogens and the development of disease according to the season (Taylor et al. 2003; Manzano et al. 2015; Migliorini et al. 2019). Year to year differences in temperature and rainfall give rise to episodic variation in disease levels over

the longer term (Harrison 1992; Peterson et al. 2015). Understanding these within- and between-year patterns is essential for effective disease management. Knowledge of how seasonal environmental factors affect infection (and other pathosystem processes) determines the best time to apply a treatment during the year. Forecasting those years in which treatment is necessary requires an understanding of the way epidemics are influenced

by temperature and moisture over extended periods (Harrison 1992).

Associations with rainfall and temperature have been particularly well studied for some forest diseases, and this knowledge has enabled the development of successful operational control programmes. A leading example is Dothistroma needle blight (DNB), a foliage disease predominantly of *Pinus* species caused by *Dothistroma septosporum* (Dorogin) M.Morelet and *Dothistroma pini* Hulbary (Bulman et al. 2016; Woods et al. 2016). The strong relationship between the incidence and severity of DNB and weather variables has been well established globally (Parker 1972; Peterson 1973; Gadgil 1974, 1977; Fraser et al. 2016; Woods et al. 2016). In a New Zealand study in which plants of radiata pine (*Pinus radiata* D.Don) were exposed weekly in the field, infection by *D. septosporum* occurred mainly between November and February (late spring to late summer), with some infection extending into April (mid-autumn; Gilmour 1981). Foliage became infected during intervals when needles remained wet for 10 or more hours at temperatures greater than 7 °C. Using extensive field data, Watt et al. (2011) found positive associations with temperature and relative humidity over the same period, as well as with November rainfall. The information from these studies explains the effectiveness of current management of DNB in forest plantations by the aerial application of a copper-based fungicide from late October, near the start of the main infection period (Gilmour & Noorderhaven 1971; Gilmour et al. 1973; Bulman et al. 2004). But severity of DNB also varies greatly between years and is closely related to the amount of yearly summer rainfall (Bulman et al. 2013). This longer-term periodicity leads to a corresponding between-year disparity in the total plantation area treated for disease, and hence in the overall annual cost (Bulman et al. 2004). Internationally, an increase in disease severity in parts of the Northern Hemisphere at the turn of the century was associated with increases in summer precipitation (Woods et al. 2005, 2016).

Research is currently underway to determine the influence of weather variables on another, more recent, foliage disease in forest plantations in New Zealand to assist in the development of a suitable treatment procedure. Red needle cast (RNC) of radiata pine and Douglas-fir (*Pseudotsuga menziesii* (Mirb.) Franco), caused by *Phytophthora pluvialis* Reeser, W.L.Sutton & E.M.Hansen, was first recognised in New Zealand in 2008 (Dick et al. 2014; Ganley et al. 2014; Hansen et al. 2015). This pathogen, taxonomically quite distinct from the true fungus *D. septosporum*, is thought to be native to the Pacific Northwest region of North America (Brar et al. 2018; Tabima et al. 2021), where it causes twig and stem cankers on tanoak (*Notholithocarpus densiflorus* (Hook. & Arn.) Manos, C.H. Cannon & S. Oh (Reeser et al. 2013) and needle cast on Douglas-fir (Hansen et al. 2015). *Phytophthora pluvialis* was recently reported in Europe for the first time, on western hemlock (*Tsuga heterophylla* (Raf.) Sarg.) in the United Kingdom (UK), causing crown dieback, defoliation, and branch and stem cankers on mature trees and mortality of young trees

(Pérez-Sierra et al. 2022). It has since been reported on Douglas-fir in Belgium (Pirronitto et al. 2024), Japanese larch (*Larix kaempferi* (Lamb.) Carrière) in the UK (Pérez-Sierra et al. 2024) and stone pine (*Pinus pinea* L.) in New Zealand (McLay et al. 2023). Red needle cast of radiata pine in New Zealand is to a lesser extent also caused by *Phytophthora kernoviae* Brasier, Beales & S.A.Kirk (Dick et al. 2014).

Much has already been learned about RNC in New Zealand pine plantations, including pathogen behaviour in relation to seasonal weather factors through the year. Symptom expression is observed largely from late autumn through winter extending into spring (Fraser et al. 2020). In a study using floating pine needles as baits, inoculum was detected predominantly in the colder months between March and December when rainfall is also plentiful (Fraser et al. 2020). In another study, plants exposed successively in the field became infected between April and September (Hood et al. 2022). The incidence and severity of RNC has also been found to vary between years and across regions in New Zealand. Although widespread nationally, certain areas, such as the Gisborne Region (referred to as Gisborne from here) in the east of the North Island, appear more prone to the disease. In parts of the country, dramatic outbreaks occur in radiata pine stands after several years without symptoms only to be succeeded by a further lull following the shedding of infected needles and growth of healthy foliage. Understanding how regional and temporal variations in weather patterns may drive these fluctuations is pertinent to effective disease management. Certain incidental empirical observations have been informative. Detections of *P. pluvialis* in diagnostics samples were greater in years following wetter and milder summers and lower following summer droughts (Fraser et al. 2020). Several instances have been noted where severe RNC expression occurred following summers with above average rainfall (Hood, unpublished data). However, the strongest evidence for the relationship between summer conditions and disease severity comes from recent large-scale analyses of disease detection via remote sensing in Gisborne (Camarretta et al. 2024; Watt et al. 2024). Greater relative humidity and rainfall, and lower solar radiation and maximum temperatures during summer, were significantly related to disease severity the following spring (Watt et al. 2024). Aligned to this, Fraser et al. (2022) found aerial spraying with cuprous oxide to be effective against RNC not only when applied during autumn, but also in summer.

These findings are consistent with the recognised epidemiology of *P. pluvialis* and *P. kernoviae*. The production of sporangia on infected needles during an epidemic, and similarity in behaviour with other airborne *Phytophthora* species, indicate that *P. pluvialis*, and likely *P. kernoviae*, undergo polycyclic lifecycles (Hood et al. 2017, 2022, Gómez-Gallego et al. 2019, Fraser et al. 2020, McLay et al. 2025). For such pathogens, the intensity of seasonal epidemics depends upon the level of initial inoculum and the rate of cyclical reinfection, both of which are affected by weather

variables (Van der Plank 1963). Although it is not yet known how *P. pluvialis* survives between outbreaks, it has been suggested that a reduction in the initial inoculum – e.g., by unfavourable hot, dry summers – may lead to lower disease levels during the following winter (Gardner et al. 2015; Fraser et al. 2020; Hood et al. 2022). Recent controlled trials have demonstrated the sensitivity of different life stages of *P. pluvialis* to warmer temperatures, at or above 23°C (McLay et al. 2025), and the importance of moisture for successful infection and sporulation (McLay et al, unpublished data). However, conditions during the subsequent autumn-winter exponential phase (the period when infection increases rapidly) may also influence the developing epidemic. Gómez-Gallego et al. (2019) found a positive correlation at several sites between mean winter relative humidity and relative abundance of *P. pluvialis* in Douglas-fir foliage. Identifying these key factors is relevant to work being undertaken to determine the time of year to apply treatments and to forecast those years in which this should be done.

To further test the hypothesis that variation in initial inoculum abundance, determined by the effect of summer weather on pathogen survival, drives between-

year differences in RNC expression, we assessed disease incidence and severity in monitoring transects across the centre and east coast of the North Island of New Zealand annually between 2015 and 2024. The data obtained also allowed for an examination of the role of weather variables during the exponential phase of epidemics, outside of summer months, in explaining between-year variation in disease expression. This dataset complements and expands on that of Watt et al. (2024) by incorporating sites across multiple regions over a longer period of ground-based monitoring. Disease data from ground and satellite (Watt et al. 2024) for nine transects enabled a direct comparison of assessment methods and conclusions between studies.

Methods

Site selection

A series of 53 RNC monitoring transects was established in radiata pine stands in the Central North Island (Bay of Plenty and Waikato Regions) and Gisborne in October 2015, during the season when generally greater disease expression is observed (Table 1; Figure 1; Figure 2).

TABLE 1: Details of red needle cast monitoring sites

| Code | Transect start ^a | Estimated stand age ^b | Transect length (m) | Elevation (m) | Stand type | <i>Phytophthora</i> identification | | |
|---------------------------------------|-----------------------------|----------------------------------|---------------------|---------------|-------------|------------------------------------|-----------------|-------------------|
| | | | | | | Pp ^c | Pk ^d | Spp. ^e |
| Central North Island sites | | | | | | | | |
| Sites with data from 2015-2023 | | | | | | | | |
| 6* | 5794382N 1877871E | Mature | 2000 | 477 | Plantation | 2022 Q&C | | 2016 |
| 10* | 5797563N 1877121E | Pre mid | 400 | 460 | Plantation | | | 2016 |
| 12* | 5785948N 1882354E | Mature | 10 | 338 | Shelterbelt | | | |
| 16* | 5779062N 1878801E | Post mid | 400 | 299 | Plantation | | | |
| 17* | 5782450N 1872014E | Pre mid | 10 | 549 | Shelterbelt | | | |
| 26* | 5758494N 1850307E | Pre mid | 200 | 380 | Plantation | 2022 Q | 2022 Q | |
| 27* | 5756736N 1859053E | Pre mid | 150 | 440 | Plantation | 2022 Q, 2023 Q | | |
| 31* | 5744025N 1833207E | Post mid | 1000 | 348 | Plantation | 2023 Q | | 2016 |
| 32* | 5713656N 1900047E | Pre mid | 1000 | 600 | Plantation | 2015 C, 2021 Q, 2022 Q&C | | |
| 33* | 5705798N 1906097E | Post mid | 1000 | 697 | Plantation | 2015 C, 2022 Q | | |
| 35* | 5727592N 1914388E | Post mid | 700 | 430 | Plantation | 2022 Q&C | | |
| 35b* | 5727592N 1914388E | Pre mid | 700 | 430 | Plantation | 2022 Q&C | | |
| 36* | 5728121N 1912292E | Pre mid | 500 | 438 | Plantation | 2018 Q&C | | |
| 37* | 5742421N 1905937E | Post mid | 600 | 533 | Plantation | 2022 Q&C, 2023 Q | | |
| 38* | 5712082N 1891176E | Mature | 1000 | 659 | Plantation | 2023 Q | | |
| Sites with data from 2015-2022 | | | | | | | | |
| 30* | 5739481N 1827878E | Post mid | 1000 | 524 | Plantation | 2022 Q&C | | 2016 |
| 34* | 5707141N 1887661E | Pre mid | 2000 | 681 | Plantation | 2015 C, 2019 Q, 2021 Q&C | | |
| Sites with data from 2015-2021 | | | | | | | | |
| 13* | 5762958N 1881973E | Post mid | 100 | 389 | Plantation | | | |
| 15* | 5762958N 1881973E | Post mid | 1300 | 399 | Plantation | | | |
| 20* | 5759720N 1853210E | Post mid | 800 | 381 | Plantation | | | |
| 28* | 5752771N 1862599E | Post mid | 150 | 298 | Plantation | | | |

TABLE 1 *continued*: Details of red needle cast monitoring sites

| Code | Transect start ^a | Estimated stand age ^b | Transect length (m) | Elevation (m) | Stand type | Phytophthora identification | | |
|---------------------------------------|-----------------------------|----------------------------------|---------------------|---------------|-------------|----------------------------------------------|-----------------|-------------------|
| | | | | | | Pp ^c | Pk ^d | Spp. ^e |
| Central North Island sites | | | | | | | | |
| Sites with data from 2015-2020 | | | | | | | | |
| 1* | 5791106N 1921987E | Post mid | 200 | 323 | Plantation | | | |
| 8* | 5798701N 1876963E | Post mid | 120 | 420 | Plantation | | | |
| 14* | 5763857N 1882184E | Post mid | 100 | 407 | Plantation | | | |
| 29* | 5750926N 1862613E | Mature | 500 | 277 | Plantation | | | |
| Sites with data from 2015-2019 | | | | | | | | |
| 7* | 5794527N 1877070E | Post mid | 10 | 495 | Plantation | | | 2015, 2016 |
| Sites with data from 2015-2017 | | | | | | | | |
| 2 | 5787719N 1919642E | Post mid | 1000 | 395 | Plantation | | | |
| 3 | 5788576N 1910849E | Mature | 2000 | 340 | Plantation | | | |
| 3a | 5788122N 1911637E | Post mid | 1000 | 341 | Plantation | | | |
| 4 | 5789352N 1910088E | Mature | 1000 | 322 | Plantation | | | |
| 5 | 5797234N 1908952E | Mature | 2000 | 132 | Plantation | | | |
| 18 | 5759297N 1853421E | Mature | 200 | 393 | Plantation | | | 2016 |
| 19 | 5759236N 1853187E | Post mid | 300 | 3918 | Plantation | | | 2015, 2016 |
| 21 | 5760675N 1851959E | Mature | 200 | 365 | Plantation | | | |
| 22 | 5760398N 1852003E | Mature | 300 | 369 | Plantation | | | |
| 23 | 5760234N 1852177E | Mature | 300 | 371 | Plantation | | | |
| 24 | 5759444N 1851563E | Post mid | 500 | 384 | Plantation | | | |
| 25 | 5759082N 1851525E | Mature | 500 | 377 | Plantation | | | |
| Sites with data from 2015-2016 | | | | | | | | |
| 9 | 5798644N 1876971E | Post mid | 200 | 420 | Plantation | | | |
| Sites with data from 2015 | | | | | | | | |
| 11 | 5789246N 1882085E | Post mid | 300 | 400 | Shelterbelt | | | |
| 39 | 5760090N 1864270E | Post mid | 600 | 519 | Plantation | | | |
| Gisborne sites | | | | | | | | |
| Sites with data from 2015-2023 | | | | | | | | |
| 40* | 5733900N 2040910E | Post mid | 100 | 544 | Shelterbelt | 2018 C, 2019 Q 2020 Q | 2019 Q | 2015 |
| 42* | 5751246N 2046788E | Post mid | 200 | 559 | Plantation | 2019 Q, 2020 Q&C | | |
| 43* | 5752097N 2046447E | Mature | 50 | 555 | Plantation | 2018 C, 2019 Q | | |
| 44* | 5752488N 2045983E | Pre mid | 200 | 575 | Plantation | 2019 Q | | |
| 45* | 5753675N 2044578E | Post mid/ mat. | 50 | 611 | Plantation | 2018 C, 2020 Q | | |
| 49* | 5751847N 2047393E | Post mid | 200 | 521 | Plantation | 2018 C, 2019 Q 2020 Q&C, 2022 Q 2023 Q | | |
| 50* | 5683009N 2020012E | Pre-mid | 500 | 474 | Plantation | 2018 C, 2020 Q&C, 2023 Q | | |
| 51* | 5683667N 2022740E | Pre-mid | 1000 | 481 | Plantation | 2018 C, 2019 Q 2020 Q | | |
| Sites with data from 2015-2022 | | | | | | | | |
| 41* | 5750312N 2046702E | Post mid | 100 | 477 | Plantation | 2018 C, 2019 Q 2020 Q | | |
| 46* | 5754891N 2043635E | Pre-mid | 30 | 602 | Plantation | | | |
| 47* | 5754746N 2043809E | Pre-mid | 150 | 600 | Plantation | 2019 Q | | |
| 48* | 5754588N 2044269E | Pre-mid/ mid | 200 | 593 | Plantation | 2018 C | | |

*Retained in data analysis; ^a New Zealand Transverse Mercator (NZTM); ^b In 2015; ^c *Phytophthora pluvialis*. Q, by high-throughput species-specific qPCR (O'Neill et al. 2018) targeting the *ypt1* or *cox2* gene region (McDougal et al. 2021; O'Neill et al. 2025); C, by isolation following the method outlined in Fraser et al. (2020); ^d *Phytophthora kernoviae*. Q, by high-throughput species-specific qPCR (O'Neill et al. 2018) targeting the *ypt1* gene region (Schena et al. 2006); ^e *Phytophthora* spp. Identified by Phytophthora ImmunoStrip (Agdia Inc., Elkhart, Indiana, USA, Cat. #92601), except site 10 for which empty sporangia were observed emerging from symptomatic needles in July 2016.

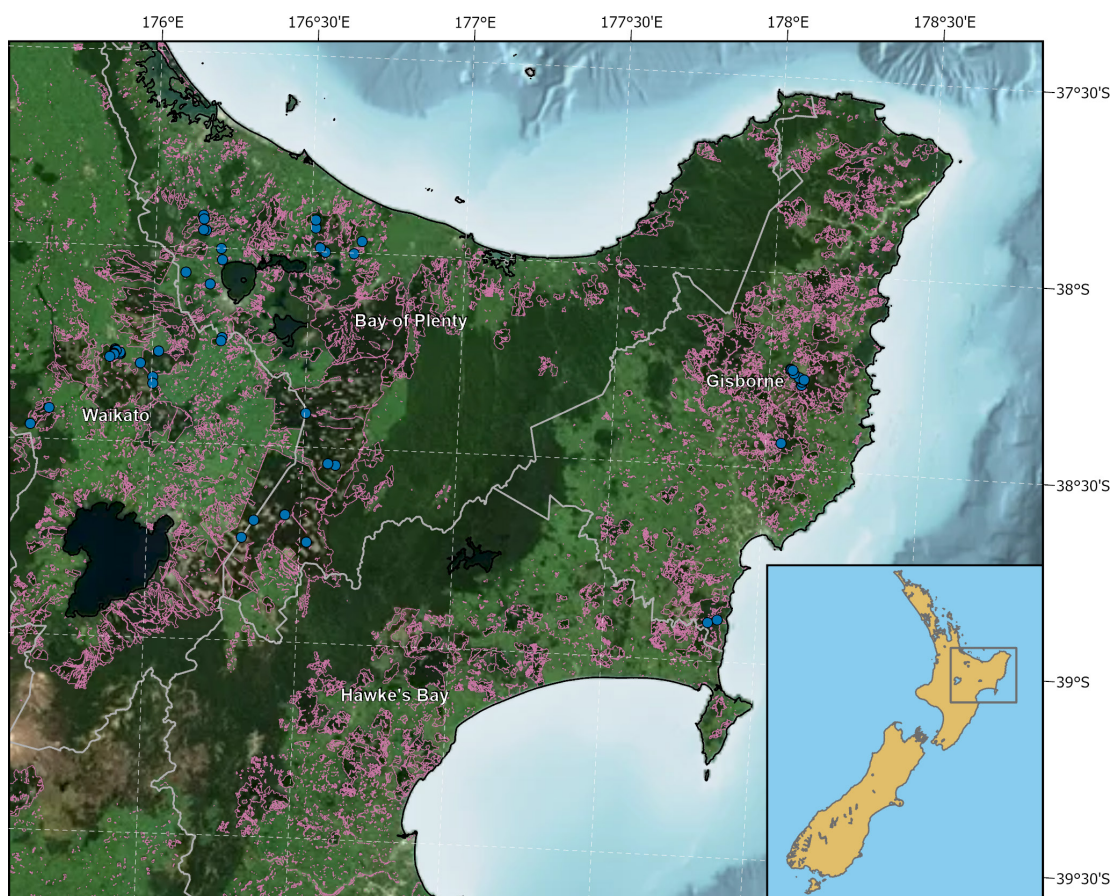


FIGURE 1: Locations of red needle cast monitoring sites (blue circles). Pink polygons indicate planted forest boundaries (Land Use and Carbon Analysis System, Ministry for the Environment, 2020 dataset). Vertical distance between Lats. 38° and 39°: 111 km. Credit: Ben Steer.



FIGURE 2: Photos of representative sites, showing variation in red needle cast severity, stand type (e.g. shelterbelt, or production plantation), stocking density and stand management.

Sites were chosen to include trees with diseased crowns, except that a small number of unaffected green stands in the Central North Island were also included for purposes of comparison. To facilitate disease assessment, each transect consisted of a length of stand edge of between 10 and 2000 m (mean 550 m) that was visible from a public or forest road. Most sites (40) were mid-rotation or later (trees approximately 12- to 25-years-old). Trees at transects in some older stands were harvested before monitoring was completed, leaving 23 sites for assessment by the end of the trial in 2023 (monitoring periods for all sites are included in Table 1). Data collected during 2024 were excluded from the analyses because of the small number of remaining sites (Table S1). At seven Central North Island sites, copper fungicide was aerially applied to control *Dothistroma* needle blight as part of routine forest management during the period of this study (or the year prior). Data from these sites for the year following application were removed from the analyses (Table S2). Only transects with a minimum of four observations were retained for data analysis (12 in Gisborne, 26 in Central North Island; Table 1).

Disease assessments

Monitoring sites were assessed for RNC levels once per year between August and October (late-winter to mid-spring), the period when disease expression is generally greatest (Dick et al. 2014; Fraser et al. 2020). At each assessment, two scores were estimated: (1) the percentage of trees along the transect length with symptoms of RNC (reddening or browning needles), to the nearest 5%; (2) the percentage of crown on the worst affected tree with symptoms of RNC, to the nearest 5%. Assessments were undertaken by three experienced Forest Pathologists, one undertaking the scoring from 2015 to 2019, one from 2017 to 2021, and one from 2021 to 2024. Assessors calibrated their scores in cross-over years.

Pathogen identification

Red needle cast symptomatology is distinctive from other pine needle diseases and disorders in New Zealand. However, care was taken to record RNC only in cases where there was no reasonable doubt. Samples were occasionally collected for laboratory verification as an additional precaution. These samples were also used to confirm whether *P. pluvialis* or *P. kernoviae* was the cause of the RNC symptoms. *Ad hoc* samples with typical RNC needle lesions were collected in polythene bags from trees within the transects or from nearby pine trees. Several different diagnostic methods were applied during the course of the study (Table 1), including Phytophthora ImmunoStrip® (Agdia, Inc., Elkhart, IN, USA, Cat. #92601), isolation following the method outlined in Fraser et al. (2020), and/or by high-throughput species-specific qPCR (O'Neill et al. 2018) targeting the *ypt1* or *cox2* gene regions (McDougal et al. 2021; Schena et al. 2006; O'Neill et al. 2025). Representative cultures from this study were deposited in Scion's National Forest Culture Collection (Table S3).

Weather data

The National Institute of Water and Atmospheric Research (NIWA) provides daily meteorological estimates for points on a Virtual Climate Station Network (VCSN) spatially interpolated using actual data from real climate stations located around New Zealand (<https://www.niwa.co.nz/climate/our-services/virtual-climate-stations>). Data for the following variables were extracted from the simulated weather station nearest to each site for the period from October 2014 to September 2023: daily maximum air temperature (°C), daily minimum air temperature (°C), daily soil temperature (°C), rain accumulation over 24 hr (mm), relative humidity (RH) at 9 am (%), solar radiation over 24 hr (MJ/m²), mean wind speed over 24 hr at 10 m (m/s), Penman's evapotranspiration index over 24 hr (kg/m²), mean sea level pressure at 9 am (hPa), vapour pressure at 9 am (hPa), and soil moisture index over 24 hr (mm).

Seasonal averages (spring: September through November; summer: December through February; autumn: March through May; winter: June through August) were computed for each variable (Table 2). Number of days with rainfall exceeding 0.3 mm and the number of days for which maximum temperature exceeded 23°C per season were also computed, as was seasonal total rain and maximum wind speed.

Impact of weather on red needle cast - statistical analysis

To elucidate weather variables that may drive RNC severity, a disease severity index, computed as the product of transect score and worst tree score divided by 100 (comparable to a percentage), was evaluated using two nonparametric statistical approaches, (1) correlation analyses and (2) a data mining technique using non-parametric binary recursive partitioning.

In the former approach, Spearman's rho, denoted r_s , which measures the strength of a monotonic (i.e. not necessarily linear) relationship between paired data, was determined. Those weather variables for which the correlation with RNC severity index was significant and at least 0.40 (in absolute terms), indicating a moderate relationship, were extracted. In the latter approach, the binary recursive partitioning technique (Breiman 2017, Breiman et al. 1984) which successively partitions data into smaller and smaller groups, each with similar characteristics, and with each split chosen to improve overall model performance, was applied. The initial dataset was randomly split into 85% training and 15% test data. The recursively partitioned regression model, using 10-fold cross-validation to determine the optimal cost complexity parameter was pruned to avoid overfitting. Pruning followed the cost complexity approach to determine the best balance between complexity and predictive accuracy. Model performance and accuracy metrics were evaluated on the test dataset. Mean absolute error (MAE) between predicted and actual values and R^2 were the chosen metrics. The pruned decision trees of the optimal model, and variable importance (normalised to a 0 - 1 scale), along with the strongest of correlations identified in the

TABLE 2: Weather variables utilised in this study, calculated from NIWA's Virtual Climate Network <https://www.niwa.co.nz/climate/our-services/virtual-climate-stations>

| Field | Units | Description |
|---------|-------------------|--------------------------------------------------------------------------------------------------------------------------------------------------------|
| avMSLP | hPa | Mean seasonal pressure reduced to Mean Sea Level in hPa AT 9am local day. |
| avPET | mm | Mean seasonal 24-hour Penman Potential Evapotranspiration total in mm FROM 9am local day. |
| avRAIN | mm | Mean seasonal total 24-hour amount of rain in mm FROM 9am local day. |
| nRain | Count | Number of rain days (>0.3 mm). |
| avRH | % | Mean seasonal relative humidity in percent AT 9am local day. |
| avSMI | mm | Mean seasonal 24-hour soil moisture index in mm FROM 9am local day calculated from rainfall and evapotranspiration ^a . |
| avETMP | °C | Mean seasonal 10cm earth temperature in °C AT 9am local day. |
| avRad | MJ/m ² | Mean seasonal 24-hour amount of accumulated global solar radiation in MJ/m ² (Mega Joules per square metre) FROM midnight local day. |
| avVP | hPa | Mean seasonal vapour pressure in hPa AT 9am local day. |
| avWIND | m/s | Mean seasonal mean wind speed in m/s at 10m above ground level over 24 hours FROM midnight local day. |
| maxWIND | m/s | Maximum wind speed within a season. |
| avTMAX | °C | Mean seasonal maximum 24-hour temperature in °C FROM 9am local day. |
| avTMIN | °C | Mean seasonal minimum 24-hour temperature in °C TO 9am local day. |
| nhot | Count | Number of days with TMAX exceeding 23 °C |

^a The base value is -150mm ("permanent wilting point") based on "soil store capacity". A value of "0" indicates the soil is at "field capacity" (amount of water held in the soil after the excess has drained away). A value greater than "0" indicates runoff.

correlation analyses, formed the basis for understanding relationships of seasonal weather with RNC disease severity.

In addition to analyses by both methods of the whole dataset comprising all sites, separate analyses were also undertaken for the Gisborne and Central North Island datasets, due to the distinctness of the regions in disease history and site characteristics.

Statistical analyses were performed using R (R Core Team 2022) supplemented by packages 'tidyverse' (Wickham et al. 2019), 'yardstick' (Kuhn et al. 2024a), 'parsnip' (Kuhn et al. 2024b), 'rsample' (Frick et al. 2024), 'rpart' (Therneau et al. 2022) and 'rpart.plot' (Milborrow 2024).

Comparison of ground based and satellite assessments

A direct comparison between the ground-based RNC index data from this study and the remote sensing RNC index of Watt et al. (2024) was undertaken for nine transects in Gisborne where data were available for both (Transects 41, 42, 45, 46, 47, 48, 49, 50, and 51). Watt et al. (2024) used Sentinel-2 satellite imagery to classify RNC severity from the difference in the normalised red/green index (R/G_{diff}) between February/March (disease free time of year) and September (peak disease). This R/G_{diff} was calculated for the pixels corresponding with the nine transects for all years that satellite imagery was available (2019-2023). Pixel values were extracted in a GIS environment (QGIS version 3.34.12) using the zonal

statistics function. For each linear transect, an internal 10-meter buffer from the forest edge was created and then used to extract pixel level information from the R/G_{diff} layers. The forest boundary layer used to match each linear transect was developed in another study and closely matched forest edges (Pearse et al. 2025). The choice of fixing the width of the transect polygon to 10 meters was made to match the resolution of the Sentinel-2 imagery used to derive the R/G_{diff} layers. The ground-based and satellite disease indices were compared by linear regression in R.

Results

General patterns of RNC expression

Red needle cast severity (index) varied among transects, regions, and years (Figure 3). Within a year and region, RNC index could vary massively among transects, from close to zero to 100 % (Figure 3). Apart from 2015, average RNC index was consistently greater for the transects in Gisborne than for those in the Central North Island (see Figure 4). In Gisborne, RNC index was least in 2015 (6 %), then increased steadily to 83 % in 2017, before declining to 7 % in 2021, followed by a rapid increase to 90 % in 2023. In the Central North Island, average RNC index was moderate from 2015-2017 (25-30 %), negligible between 2018 and 2021, and greatest in 2023 (43 %). RNC was low (4 %) in both regions in 2024 (Table S1).

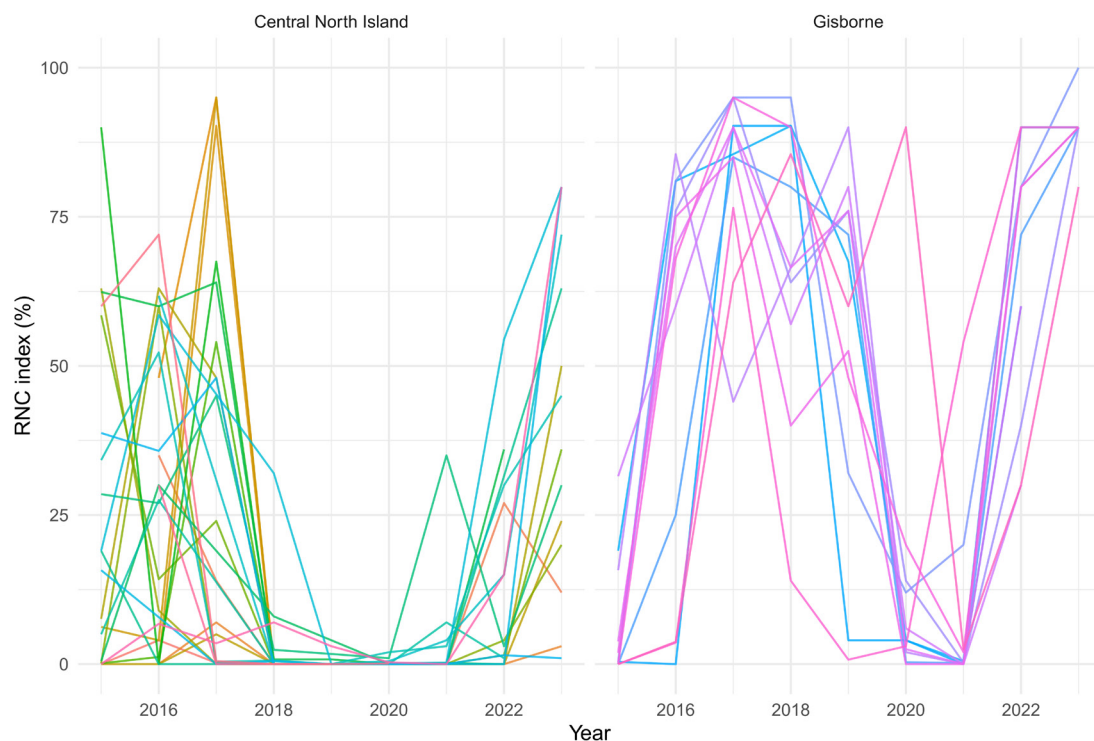


FIGURE 3: Annual red needle cast index at each monitoring transect in the Central North Island and Gisborne Region. Different transects are represented by different coloured lines.



FIGURE 4: Annual averages of regional red needle cast severity (%) and key seasonal weather variables identified through correlation and binary recursive partitioning analyses. CNI, Central North Island.

Pathogen identification

Phytophthora pluvialis was confirmed as the dominant cause of RNC at the study sites. Across all years, *P. pluvialis* was confirmed present at 11/12 transects in Gisborne and 11/15 transects in the Central North Island that survived until the end of monitoring (Table 1). *Phytophthora kernoviae* was detected at two transects: one in Gisborne in 2019 and another in the Central North Island in 2022, both times co-occurring with *P. pluvialis*.

Spearman correlations of RNC index and seasonal weather variables

With data from all transects, RNC index significantly correlated with seven weather variables ($|r_s| \geq 0.40$): four from autumn, two from summer, and one from winter (Table 3). RNC index was positively correlated to autumn mean vapour pressure, mean minimum temperature, mean soil temperature, and number of rain days (see also Figure 4). RNC index was negatively correlated to summer mean maximum temperature (Figure 4) and number of hot days ($>23^\circ\text{C}$), as well as winter mean relative humidity.

When the two regions were analysed separately, different weather variables of importance emerged compared to the analysis of the full dataset. There was no agreement (amongst variables for which the absolute value of the correlation was at least 0.40) between the Gisborne and Central North Island datasets. A greater number of variables significantly correlated with disease in Gisborne, and stronger relationships were seen for this dataset (Table 3).

For the Gisborne dataset, RNC index significantly correlated ($|r_s| \geq 0.40$) with 11 weather variables: six from autumn, three from spring, one from summer, and one from winter. The strongest correlation, a positive relationship, was with autumn mean soil moisture index (0.70; Figure 4). Autumn mean minimum temperature (0.57), mean vapour pressure (0.55), number of rain days (0.49) and mean relative humidity (0.44) were all also positively correlated with RNC index (see also Figure 4). Autumn maximum wind was negatively correlated with disease (-0.51). Spring mean evapotranspiration

(-0.58) was negatively correlated with RNC index. Spring mean relative humidity (0.47) and mean soil moisture index (0.41) were positively correlated with RNC index. Summer maximum wind (0.53) was positively correlated with disease. Winter mean sea level pressure (-0.56) was negatively correlated with RNC index.

For the Central North Island dataset, RNC index significantly correlated ($|r_s| \geq 0.40$) with four weather variables, the strongest relationship being with autumn mean evapotranspiration (-0.46). Two summer variables, mean evapotranspiration (-0.40) and mean maximum temperature (-0.40; Figure 4), were negatively correlated with RNC index. Winter mean vapour pressure was negatively correlated with RNC index (-0.42).

Binary recursive partitioning analysis of disease index and seasonal weather variables

When data for all transects were analysed by binary recursive partitioning, four autumn, four winter, and two spring variables made up the top ten most important weather factors in explaining RNC index (Figure 5). With just three splits, model performance assessed using the test dataset was $R^2 = 0.55$, $MAE = 17.4\%$. Autumn mean vapour pressure was by far the most important variable (normalised importance = 0.19). Spring mean soil temperature, autumn mean soil temperature, autumn mean minimum temperature, and spring mean vapour pressure followed with similar normalised importance measures (0.09 – 0.11). Four winter variables—maximum wind, mean relative humidity, mean wind, and mean sea level pressure—along with autumn maximum wind were also amongst the top 10 (normalised variable importance 0.04 – 0.07). The most important summer variable was mean sea level pressure (11th with a normalised importance of 0.04). The model predicted moderate RNC index (averaging 54 %) when autumn mean vapour pressure was at least 13 hPa and low RNC index (13 %) at lower vapour pressures. The greatest RNC index (70 %) was associated with autumn mean vapour pressure of at least 13 hPa and winter maximum wind of less than 8.6 (m/s).

TABLE 3: Spearman correlations (for which $|r_s| \geq 0.40$) of red needle cast index and seasonal weather variables. Highlighted variables are consistent across datasets. Identical variables share the same colour.

| All transects | r_s | Central North Island | r_s | Gisborne Region | r_s |
|---------------|-------|----------------------|-------|-----------------|-------|
| avRH_Winter | -0.50 | avPET_Autumn | -0.46 | avSMI_Autumn | 0.70 |
| avVP_Autumn | 0.50 | avVP_Winter | -0.42 | avMSLP_Winter | -0.58 |
| avTMIN_Autumn | 0.48 | avPET_Summer | -0.40 | avPET_Spring | -0.58 |
| avTMAX_Summer | -0.44 | avTMAX_Summer | -0.40 | avTMIN_Autumn | 0.57 |
| nrain_Autumn | 0.44 | | | avVP_Autumn | 0.55 |
| nhot_Summer | -0.41 | | | maxWIND_Summer | 0.53 |
| avETMP_Autumn | 0.40 | | | maxWIND_Autumn | -0.51 |
| | | | | nrain_Autumn | 0.49 |
| | | | | avRH_Spring | 0.47 |
| | | | | avRH_Autumn | 0.43 |
| | | | | avSMI_Spring | 0.41 |

The binary decision tree for Gisborne transects identified two autumnal splits segregating RNC index into low, moderate, and high severity (Figure 6). RNC index was predicted to be low (averaging 7 %) when autumn mean soil moisture index was below -54 mm. At wetter levels of mean soil moisture, RNC index was predicted to be moderate (32 %) when autumn mean vapour pressure was less than 12 hPa, and high (74 %)

when 12 hPa or greater. Goodness-of-fit statistics for the test dataset were $R^2 = 0.63$, and MAE = 18.1 %. As identified with correlation analyses, autumn mean soil moisture index was the most important variable (with a normalised importance of 0.20). Spring mean relative humidity (0.19), spring mean evapotranspiration (0.15), summer mean relative humidity (0.13), summer mean soil moisture index (0.11), and winter mean sea

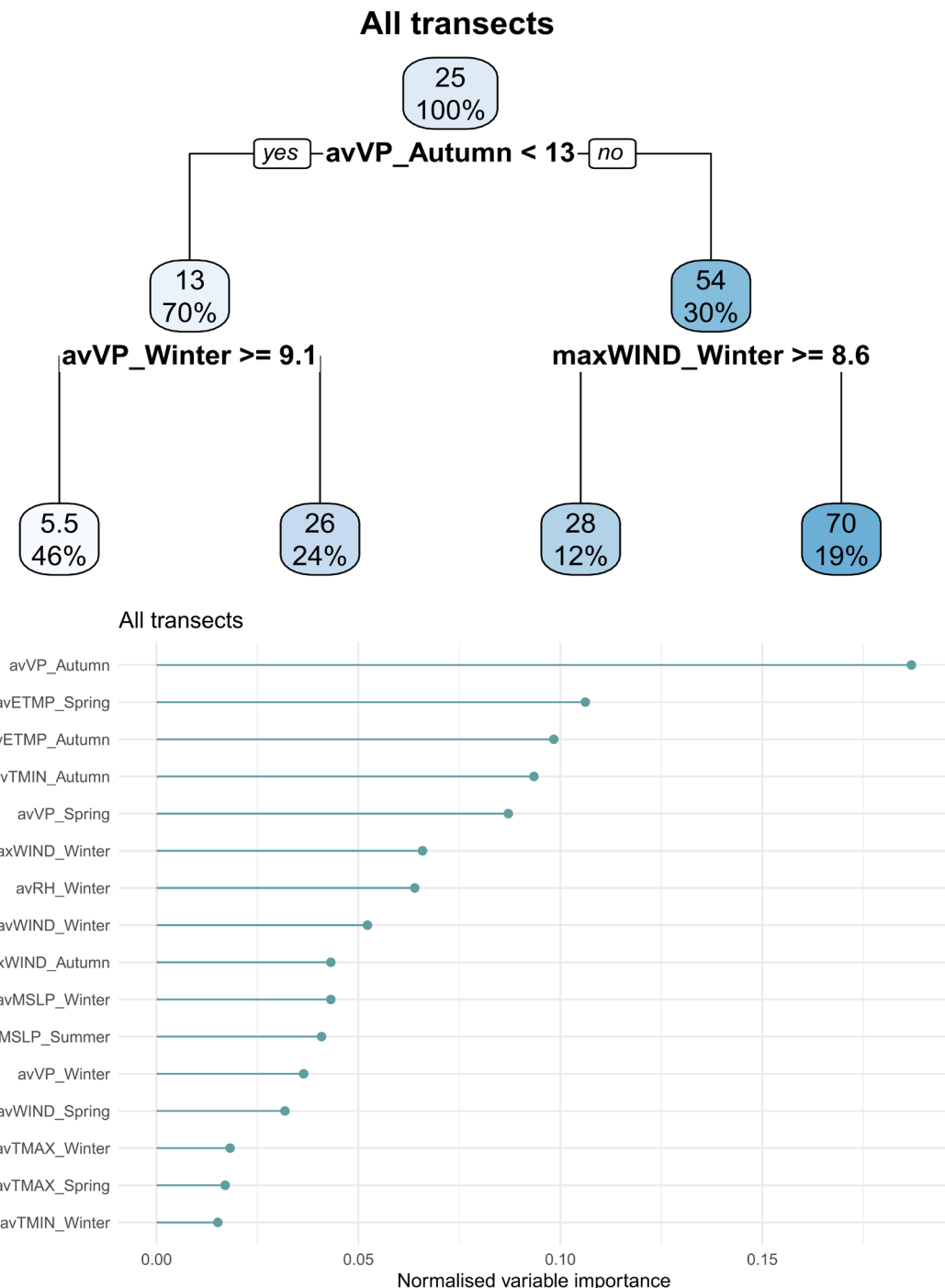


FIGURE 5: Binary recursive partitioning analysis, showing decision tree and variable importance, of seasonal weather impacts on red needle cast index for all transects. Upper numbers in the shaded polygons give mean RNC index estimates (%), lower numbers indicate the percentage of data points.

level pressure (0.11) followed in terms of importance. The remaining variables in the top 10 but with lesser importance (< 0.03) were: mean vapour pressure for each of the four seasons (autumn > spring > winter > summer) and spring number of hot days.

The decision tree for the Central North Island (Figure 7) had three splits comprising two autumn (mean vapour pressure and mean minimum temperature)

and one winter variable (mean vapour pressure). Goodness-of-fit statistics for the test dataset were $R^2 = 0.68$, and $MAE = 7.8\%$. RNC index was low (averaging 10 %) at autumn mean vapour pressures less than 13 hPa. RNC index was greatest (65 %) when autumn vapour pressure was greater than 13 hPa and autumn mean minimum temperature less than 9.4°C. The most important variable was autumn mean vapour pressure

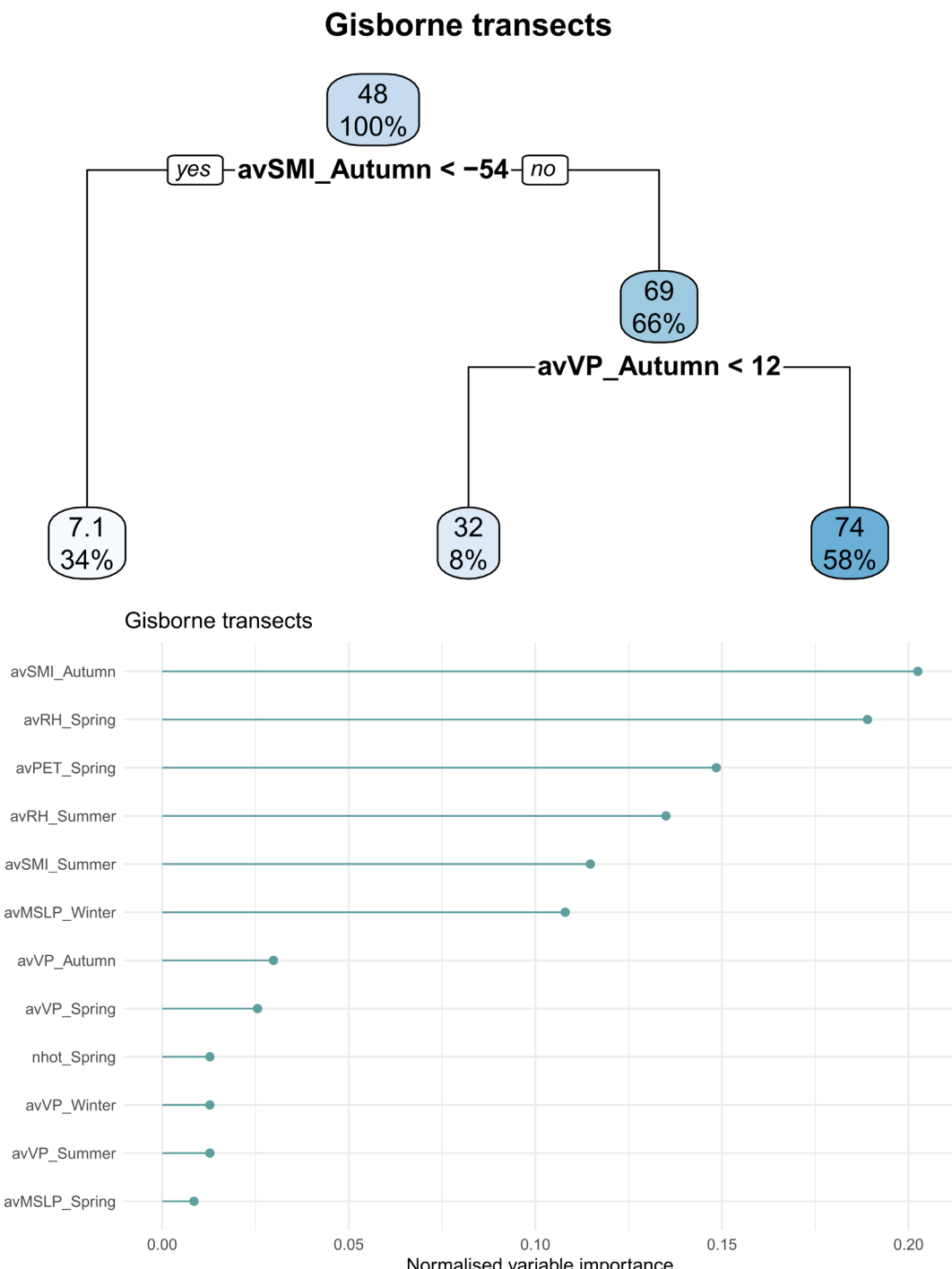


FIGURE 6: Binary recursive partitioning analysis of seasonal weather impacts on red needle cast index for transects in the Gisborne Region. Upper numbers in the shaded polygons give mean RNC index estimates (%), lower numbers indicate the percentage of data points.

with a normalised importance of 0.15 followed by autumn mean minimum temperature (0.12) and spring mean radiation (0.11). The six variables that followed were of similar importance (0.07): autumn mean soil temperature, winter mean vapour pressure, winter mean

sea level pressure, winter mean radiation, winter mean wind, and summer mean minimum temperature. Winter mean minimum temperature completed the top 10 list (0.04). All remaining variables identified as important (Figure 7) had lower normalised values (down to 0.02).

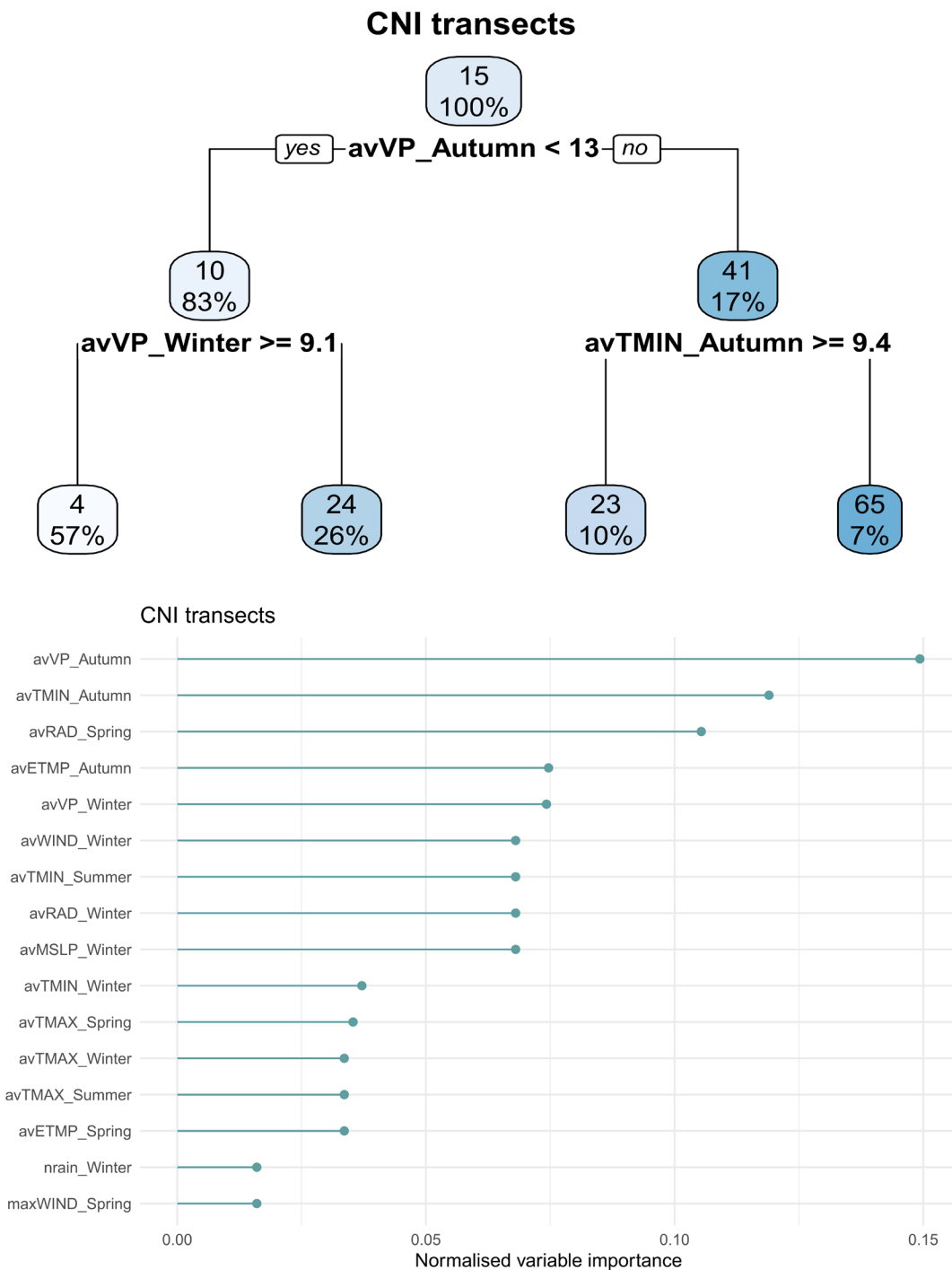


FIGURE 7: Binary recursive partitioning analysis of seasonal weather impacts on red needle cast index for transects in the Central North Island (CNI). Upper numbers in the shaded polygons give mean RNC index estimates (%), lower numbers indicate the percentage of data points.

Comparison of ground-based and satellite assessments

Ground-based and remote sensing RNC estimates for the nine transects were significantly positively related ($R^2 = 0.54$, $F(1, 39) = 45.9$, $p < 0.001$; Figure 8). Comparing yearly averages, including regional estimates from Watt et al. (2024) as well as transect-specific estimates, there was good agreement between all three datasets, with the greatest disease levels in 2023, intermediary levels in 2019 and 2022, and the lowest levels in 2020 and 2021 (Figure 8).

Discussion

There was significant variation in red needle cast incidence and severity within- and among- sites, regions, and years. Generally, disease expression was

more common and severe at sites in Gisborne than the Central North Island. In both regions, mean annual RNC oscillated between peaks in 2017 and 2023, with lows between 2018 and 2021 (more pronounced in the Central North Island). Within sites, RNC expression could vary vastly between years, but could also express consistently (more so in Gisborne). *Phytophthora pluvialis* was found to be the species most associated with RNC, corresponding with the findings of previous studies. Results did not unequivocally support the hypothesis that summer weather, through its impact on pathogen survival and initial inoculum levels, drives between-year variation in RNC expression. Weather conditions during seasons outside of summer, particularly autumn, when exponential epidemic growth is more likely to occur, appeared to have a greater impact on disease severity. While variables from all seasons

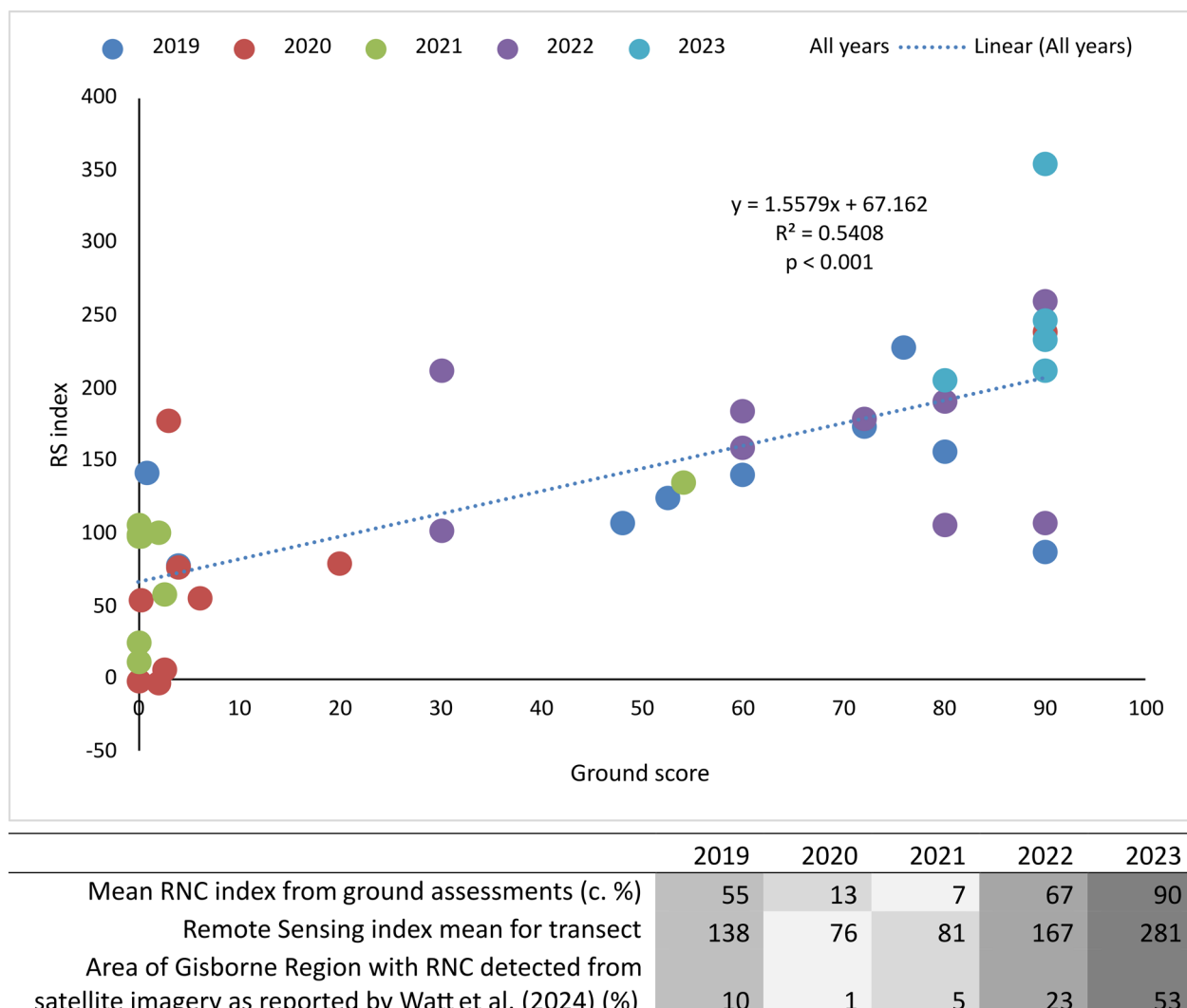


FIGURE 8: Relationship between red needle cast index from ground scores and remote sensing index for nine sites in the Gisborne Region. Ground scores were calculated as transect score \times worst tree / 100 (translating to a rough percentage canopy affected). The RS index is the differences in Red/Green indices from September and February/March each year (R/G_{diff}). The table also includes data estimated for the whole region from Watt et al. (2024). Degree of shading in the table indicates rank of RNC severity (light grey = low disease, dark grey = severe disease).

were found to have relationships with RNC expression, and the most important variables differed between the two regions, autumn and spring variables tended to have the strongest correlations with disease and greatest importance. When data for all transects were analysed together, autumn mean vapour pressure, a measure of atmospheric humidity, was the most important variable by both analysis methods (positively related to RNC). When the Gisborne dataset was analysed separately, autumn mean soil moisture index, which incorporates current and prior rainfall and evapotranspiration, was the most important variable by both analysis methods (positively related to RNC). When the Central North Island dataset was analysed separately, autumn mean vapour pressure (positive relationship) was the most important variable by binary recursive partitioning analysis, but autumn mean evapotranspiration (negative relationship) had the strongest correlation.

While numerous seasonal weather variables have potential importance in determining RNC severity, care must be taken interpreting the impact of individual weather variables on RNC, given their co-variation. There was also variation between the two regions in weather variable importance, with greater complexity in relationships seen in the Central North Island. However, relationships between weather variables and RNC were generally as expected based on previous knowledge of the pathosystem: RNC tended to be greater following wetter weather (greater vapour pressure, relative humidity, rainfall, soil moisture index; lower evapotranspiration) and milder temperature conditions (dependent on season, lower maximum temperatures and hot days in summer, greater minimum (and soil) temperatures in autumn). These relationships correspond with the known moisture and temperature requirements of the different life stages of *P. pluvialis*. Needle wetness is required for both infection and sporulation (McLay et al. unpublished data). Controlled studies have also demonstrated the direct impact of temperature on several *P. pluvialis* life stages; with infection and sporulation greatest between 10–20°C and restricted at or above 23°C (McLay et al. 2025). These relationships may explain the contrasting role between seasons of maximum and minimum temperature. Generally, in the regions studied here, temperatures warm enough to limit *P. pluvialis* are restricted to summer months, while in other months, rates of infection and sporulation will increase with minimum temperature, if moisture is also available. Further, numerous prior field studies have demonstrated similar relationships between the weather variables identified here and a range of RNC metrics. Detection of *P. pluvialis* inoculum in the same two regions was positively related to moisture variables and negatively related to maximum temperature (Fraser et al. 2020). Infection by *P. pluvialis* and *P. kernoviae* on trap plants in the Central North Island occurred predominantly during periods of the year when temperatures, solar radiation, and evapotranspiration are lowest, relative humidity is greatest, and rainfall is plentiful (Hood et al. 2022). Abundance of *P. pluvialis* in foliage of Douglas-fir was positively related to site

winter relative humidity (Gómez-Gallego et al. 2019). Annual RNC severity in Gisborne, as measured from satellite imagery, was positively related to rainfall and relative humidity and negatively related to radiation and maximum air temperature in mid- to late-summer (Watt et al. 2024).

Superficially, the finding that autumn vapour pressure in the Central North Island and soil moisture index in Gisborne were the most important weather variables in explaining annual RNC expression contrasts to the results of Watt et al. (2024), who posited that between-year survival of the pathogen, driven by summer conditions, was critical in determining annual variation in disease expression. Autumn soil moisture index, calculated from cumulative rainfall and evapotranspiration, will be directly impacted on by the variables identified by Watt et al. (2024), suggesting that there is some agreement between the studies. However, the findings reported here imply that the cumulative effect of weather variables that impact moisture and temperature during a longer period from late summer through autumn are important, and thus that conditions during the exponential epidemic phase play a significant role in RNC expression. Soil moisture index was not included in the analysis by Watt et al. (2024), so a direct comparison of the studies cannot be made. It is important to note that although not the most important variables, summer relative humidity and soil moisture index for the Gisborne dataset, and summer mean minimum temperature for the Central North Island dataset were also identified as important variables. Likewise, summer mean maximum temperature and number of hot days (maximum temperature $>23^{\circ}\text{C}$) for the complete dataset, and summer mean maximum temperature and evapotranspiration for the Central North Island dataset were moderately negatively correlated to RNC severity.

The two variables identified as most important in this study, autumn vapour pressure and soil moisture index, most likely impact RNC severity indirectly through their co-variation with other weather variables, rather than having direct impact on disease processes. Vapour pressure is the contribution of water vapour to atmospheric pressure. When temperature is held constant, an increase of vapour pressure means an increase in humidity. Greater humidity will increase condensation and dew formation, supporting pathogen infection, sporulation, and spread. However, vapour pressure in this dataset was strongly positively correlated with temperature variables, particularly minimum temperature (data not shown). Thus, the positive relationship between autumn vapour pressure and RNC severity may also be linked to minimum temperatures. Greater minimum temperatures, when maximum temperatures and moisture availability are not limiting, may increase rates of infection and sporulation (McLay et al. 2025). Greater minimum temperatures may also indicate periods of cloudy weather, in contrast to lower minimums associated with clear skies. The relationship between RNC severity and soil moisture index, calculated from rainfall and evapotranspiration, is easier to explain, as this variable likely correlates strongly with pathogen

infection, sporulation, and spread risk. Free moisture on foliage and moderate temperatures ($<23^{\circ}\text{C}$) are critical for all three of these disease processes (McLay et al. 2025; McLay et al. unpublished data). Soil moisture index is negatively correlated with temperature variables, evapotranspiration, and radiation and positively correlated with rainfall and relative humidity. The strength of its importance likely results from its cumulative nature, representing accrued risk of multiple cycles of infection, sporulation, and spread by the pathogens during late summer and through autumn, the latter season being a time when maximum temperatures will no longer be limiting. Aligned to this, the finding that spring variables (9–12 months before disease assessments) were of importance in several analyses indicates that a long cumulation of conditions impacting pathogen survival and population growth may be playing a role. Similar findings have been reported for *Phytophthora ramorum* Werres, De Cock & Man in't Veld in forests in Oregon, where extent of disease was best explained by spring precipitation and extent of disease the year prior (Peterson et al. 2015).

The effects of weather on infection and sporulation appear to extend indirectly beyond the current year. In this study, despite variation among sites in annual trends, disease severity at the regional scale rose steadily over several years to the peaks in 2017 and 2023, with a corresponding decrease to a trough during the interval between (Figure 4). The amount of initial inoculum each season may depend on the level of disease during the previous year. It is not yet known how *P. pluvialis* survives between years, but it is likely that favourable weather leading to extensive disease results in increased primary inoculum in the following year. Repetition causes a progressive increase in disease severity over several successive years until there is an inevitable collapse or decline as most inoculum is lost with the shedding of infected foliage from much of the crown.

The trend in RNC expression seen for the sites in Gisborne corresponded well with those reported by Watt et al. (2024) for the whole region indicating that, despite assessing a limited number of sites in this study, the results are representative of larger-scale regional trends in disease expression. For nine sites, a direct comparison between ground and aerial scores was possible allowing evaluation of the sensitivity of the remote sensing classification. Watt et al. (2024) classified a R/G_{diff} lower than 200 as healthy, between 200–280 as low severity, 280–380 as medium severity, and above 380 as high severity RNC. Although the ground and aerial scores were positively correlated (Figure 8), there was an indication that the remote sensing classifications may underestimate disease or that the ground-based disease index may inflate disease severity, or both. This is not unexpected, given disease will likely have to express higher in the crown for aerial detection and the ground-based index, derived from the complete crown depth, may inflate disease in cases when small amounts of symptoms are present on many trees combined with one or a few trees with severe expression. The discrepancy between assessment methods may somewhat explain

the variation between the studies in identifying seasonal weather variables of importance. The method of Watt et al. (2024) may only be detecting the severest disease, which largely occurred in 2022 and 2023, years that coincided with extreme mid- to late-summer rainfall events. The shorter monitoring period of Watt et al. (2024) (5 years) compared to this study (9 years) may also partially explain the discrepancy in findings. Further ground truthing will be needed to better relate the remote sensing index to on-ground severity. This may be important for work that aims to enable regional scale estimates of RNC growth impacts by determining the relationship between remote sensing severity classifications and growth impacts. Nonetheless, these comparisons provide confidence that either method can be used to distinguish years of severe or little disease to support identification of environmental drivers.

Improving our understanding of regional and site variation in disease expression was not the focus of this study, however the results demonstrate that expression of RNC was greater and more consistent at sites in Gisborne than the Central North Island. This is similar to the pattern seen previously for detection of inoculum at a small number of sites in each region (Fraser et al. 2020). In that study, inoculum of *P. pluvialis* was detected in all three years at all sites in Gisborne but only in one year at a site in the Central North Island. Several factors may have contributed to this regional variation, including differences in weather, site factors, and management operations (see below). All sites in Gisborne were located in coastal high elevation plantations (c. 500–600 m asl) and thus were exposed to more maritime weather conditions, with greater seasonal total rain, fewer hot days, and warmer mean seasonal minimum temperatures (Table 4), that together may have increased pathogen survival and disease development rates.

The difference in expression between these regions may also be linked to variation in *Dothistroma* needle blight (DNB) presence and management. In the Central North Island, low volumes of cuprous oxide are aerially applied to control DNB. Aerial surveys are undertaken in July and August and plantations under 16 years of age with symptomatic foliage percentages above certain thresholds are identified for control operations that take place in November and February (Bulman et al. 2004). The disease is rarely confirmed by ground truth, and therefore, it is likely that these applications may be providing some control of RNC in these areas. In contrast, DNB is less commonly reported in Gisborne, where no active control programmes are currently in place. Cuprous oxide, applied at the same dose as that used for DNB control, is known to reduce RNC incidence and severity at an operational level (Fraser et al. 2022). It is possible that these operations are partly responsible for the lower levels of RNC observed in the Central North Island and they may have impacted our conclusions on the role of weather. Application of cuprous oxide may reduce *P. pluvialis* inoculum loads in the region, impacting sites that may not have been treated directly. During this study, control operations were carried out in stands adjacent to our sites in several years and cuprous

TABLE 4: Mean seasonal weather variables for the study sites in the two regions. Sites in the Gisborne region were in coastal high elevation plantations, exposed to more maritime weather conditions, with greater seasonal total rain, fewer hot days, and warmer mean seasonal minimum temperatures (bold).

| Region | Season | MSLP | PET | RAIN | RH | SMI | ETMP | RAD | TMAX | TMIN | VP | WIND | max WIND | sum RAIN | nrain | Nhot |
|----------|--------|------|-----|------|------|-------|------|------|------|-------------|------|------|----------|------------|-------|-------------|
| CNI | Spring | 1016 | 2.8 | 4.1 | 80.9 | -18.4 | 12.1 | 16.2 | 16.4 | 7.0 | 11.4 | 3.9 | 13.1 | 369 | 37.3 | 2.2 |
| | Summer | 1016 | 4.2 | 3.5 | 77.5 | -73.1 | 18.3 | 21.1 | 22.5 | 11.9 | 15.3 | 3.6 | 13.5 | 314 | 25.7 | 38.7 |
| | Autumn | 1018 | 1.8 | 4.1 | 87.8 | -41.1 | 13.1 | 11.5 | 18.0 | 8.2 | 12.8 | 3.2 | 11.5 | 379 | 30.0 | 5.8 |
| | Winter | 1017 | 0.8 | 4.9 | 90.4 | 1.5 | 7.0 | 7.4 | 12.2 | 3.5 | 9.2 | 3.5 | 12.0 | 450 | 38.4 | 0.0 |
| Gisborne | Spring | 1015 | 3.3 | 5.0 | 77.2 | -25.6 | 13.3 | 17.8 | 16.5 | 8.2 | 11.6 | 4.1 | 10.8 | 450 | 34.8 | 1.7 |
| | Summer | 1015 | 4.5 | 3.4 | 76.4 | -82.1 | 19.7 | 22.1 | 21.6 | 12.8 | 15.6 | 3.8 | 12.9 | 307 | 27.1 | 28.1 |
| | Autumn | 1018 | 2.2 | 4.8 | 83.4 | -34.6 | 13.8 | 11.7 | 18.0 | 9.9 | 13.2 | 3.5 | 10.5 | 440 | 34.8 | 4.1 |
| | Winter | 1016 | 1.3 | 5.7 | 83.7 | -0.3 | 7.7 | 7.9 | 12.9 | 5.5 | 9.4 | 3.9 | 10.7 | 523 | 40.2 | 0.0 |

oxide was directly applied to at least seven study sites in the Central North Island (Table S2). Data for the year following direct control operations were removed from the analysis. Three sites were treated in one year and four sites in two years during (or immediately preceding) the monitoring window. RNC severity in the year of, and year immediately following, spray application varied from low to moderate. Two instances of moderate disease development the year after application contrasts with the results of Fraser et al. (2022), who found that application of cuprous oxide in November reduced RNC severity the year following. Although this study was not designed to test this element, the observation may indicate research on efficacy and optimal spray timing for control of RNC may be required on a wider range of sites.

Regardless of the cause of regional differences in disease expression and weather variables of importance, it suggests there may be a need for site- or region-specific monitoring and management of RNC. There are other examples of *Phytophthora* species being limited by different processes in contrasting areas. For example, seasonality of *P. kernoviae* sporulation varies between New Zealand and the UK (Fraser et al. 2020). Detection of inoculum peaked in the cooler and wetter winter months in New Zealand, but in the warmer and drier summer months in the UK. Warmer summer temperatures in New Zealand, that reached above thresholds for successful infection, likely limited the pathogen there, while cooler winter temperatures likely limited the pathogen in the UK. Similarly, activity of *P. ramorum* is primarily limited by cold winter weather in the UK but by hot summer weather in California (Garbelotto & Hayden 2012). At a smaller scale, Swiss needle cast (*Nothophaeocryptopus gaeumannii*) impact on Douglas-fir in Oregon was shown to more strongly relate to winter conditions at wetter, cooler sites, but summer conditions at drier, warmer sites (Lee et al. 2013). Similar variation likely occurs between regions of New Zealand, which incorporate significant gradients in temperature and moisture variables. Development of process-based epidemiological models for *P. pluvialis*, currently underway using data from controlled environment experiments (McLay et al.

2025), may have an advantage over empirical models, such as those developed here, in allowing predictions of RNC risk across a range of regions, time periods, and climate scenarios not yet experienced (Cunniffe & Gilligan 2020).

Our results have critical implications for the development of RNC control programmes. The importance of autumn, more than summer weather variables in determining annual disease severity indicates that proactive control activities may require long-term weather forecasting or frequent monitoring. Application of cuprous oxide in November, February, or April/May has been shown to reduce RNC in one trial series in the Central North Island (Fraser et al. 2022). If annual RNC emergence could be predicted at the end of summer (Watt et al. 2024), this would allow application of effective control in autumn. As forest disease control operations are logically demanding and dependent on international supply chains, delayed disease predictions will challenge the development of control programmes.

Conclusions

The results reported here show that annual red needle cast expression is largely explained by autumn weather. Autumn vapour pressure and soil moisture index were the most important variables in the Central North Island and Gisborne Regions, respectively. The importance of autumn more than summer weather variables in determining disease contrasts with the findings of previous studies and indicates that proactive control activities may require long-term weather forecasting or frequent monitoring. Variation between regions in disease history and the importance of different weather variables suggest that site-specific RNC management may be required, and that the development of process-based epidemiological models may be advantageous over data driven (empirical) models. It is hoped that the results reported here will contribute to the further development of an integrated disease management programme for RNC.

Competing interests

The authors declare that they have no competing interests.

Authors' contributions

Conception, study design and establishment of monitoring sites: IH; Data Capture: IH, SF, EM, NC; Data analysis: CT; Drafting of manuscript: SF, IH, CT; Contribution to and editing of manuscript: all; Project supervision and administration: IH, SF, EM.

Acknowledgements

This work formed part of the Needle Disease Control Strategy and the Resilient Forests Programme, both funded by the Forest Growers Levy Trust and Scion's Strategic Science Investment Funding (from the Ministry of Business, Innovation & Employment). We are thankful to Judy Gardner for early input into project planning and to Catherine Banham, David Lane, Andrew Pugh, Mike Davy, Kat Wardhaugh, and Gordon Tieman who provided technical assistance with data collection. We thank Ben Steer for production of Figure 1. Forest owners and managers are thanked for allowing access to study sites and for providing disease management histories. We are thankful to Michael Bartlett, Hazel Daniels and Peter Clinton for reviewing a prior draft of the manuscript and to Horacio Bown, Dave Shaw and two anonymous reviewers for their constructive feedback that improved the manuscript.

References

Brar, S., Tabima, J.F., McDougal, R.L., Dupont, P.Y., Feau, N., Hamelin, R.C., Panda, P., LeBoldus, J.M., Grünwald, N.J., Hansen, E.M., Bradshaw, R.E., & Williams, N.M. (2018). Genetic diversity of *Phytophthora pluvialis*, a pathogen of conifers, in New Zealand and the west coast of the United States of America. *Plant Pathology*, 67, 1131-1139. <https://doi.org/10.1111/ppa.12812>

Breiman, L. (2017). *Classification and regression trees*. Routledge. <https://doi.org/10.1201/9781315139470>

Breiman, L., Friedman J.H., Olshen R.A., & Stone C.J. (1984). *Classification and regression trees*. Chapman and Hall.

Bulman, L.S., Gadgil, P.D., Kershaw, D.J., & Ray, J.W. (2004). *Assessment and control of Dothistroma needle blight*. Forest Research Bulletin No. 229. Rotorua, New Zealand: New Zealand Forest Service, Forest Research Institute. http://www.nzfoa.org.nz/images/stories/pdfs/content/fhrc_reports/2002-01.pdf

Bulman, L.S., Dick, M.A., Ganley, R.J., McDougal, R.L., Schwelm, A., & Bradshaw, R.E. (2013). Dothistroma needle blight. In P. Gonthier & G. Nicolotti (Eds.), *Infectious forest diseases* (pp. 436-457). Boston, MA: CABI. <https://doi.org/10.1079/9781780640402.0436>

Bulman, L.S., Bradshaw, R., Fraser, S., Martín-García, J., Barnes, I., Musolin, D., La Porta, N., Woods, A., Diez, J., Koltay, A., Drenkhan, R., Ahumada, R., Poljakovic-Pajnik, L., Queloz, V., Piškur, B., Doğmuş-Lehtijärvi, H., Chira, D., Tomešová-Haataja, V., Georgieva, M., Jankovský, L., Anselmi, N., Markovskaja, S., Papazova-Anakieva, I., Sotirovski, K., Lazarević, J., Adamčíková, K., Boroň, P., Bragança, H., Vetraino, A., Selikhovkin, A., Bulgakov, T., & Tubby, K. (2016). A worldwide perspective on the management and control of Dothistroma needle blight. *Forest Pathology*, 46, 472-488. <https://doi.org/10.1111/efp.12305>

Camarretta, N., Pearse, G.D., Steer, B.S.C., McLay, E., Fraser, S., & Watt, S. (2024). Automatic detection of *Phytophthora pluvialis* outbreaks in radiata pine plantations using multi-scene, multi-temporal satellite imagery. *Remote Sensing*, 16, 338. <https://doi.org/10.3390/rs16020338>

Cunniffe, N.J., & Gilligan, C. A. 2020. Use of mathematical models to predict epidemics and to optimize disease detection and management (Chapter 12). In J.B. Ristaino & A. Records (Eds.), *Emerging plant diseases and global food security* (pp. 239-266). APS Press, St. Paul, MN, USA. <https://doi.org/10.1094/9780890546383.012>

Dick, M.A., Williams, N.M., Bader, M.K.-F., Gardner, J.F., & Bulman, L.S. (2014). Pathogenicity of *Phytophthora pluvialis* to *Pinus radiata* and its relation with red needle cast disease in New Zealand. *New Zealand Journal of Forestry Science*, 44: 6. <https://doi.org/10.1186/s40490-014-0006-7>

Fraser, S., Mullett, M.S., Woodward, S., & Brown, A.V. (2016). Between-site and-year variation in the relative susceptibility of native Scottish *Pinus sylvestris* populations to Dothistroma needle blight. *Plant Pathology*, 65, 369-379. <https://doi.org/10.1111/ppa.12425>

Fraser, S., Gómez-Gallego, M., Gardner, J., Bulman, L.S., Denman, S., & Williams, N.M. (2020). Impact of weather variables and season on sporulation of *Phytophthora pluvialis* and *Phytophthora kernoviae*. *Forest Pathology*, 50: e12588. <https://doi.org/10.1111/efp.12588>

Fraser, S., Baker, M., Pearse, G., Todoroki, C., Estarija, H.J., Hood, I.A., Bulman, L.S., Somchit, C., & Rolando, C.A. (2022). Efficacy and optimal timing of low volume aerial applications of copper fungicides for the control of red needle cast of pine. *New Zealand Journal of Forestry Science*, 52: 18. <https://doi.org/10.33494/nzjfs522022x211x>

Frick H., Chow F., Kuhn M., Mahoney M., Silge J., & Wickham H. (2024). *rsample: General resampling infrastructure*. [R package version 1.2.1]. <https://CRAN.R-project.org/package=rsample>. Accessed 14 March 2025.

Gadgil, P.D. (1974). Effect of temperature and leaf wetness period on infection of *Pinus radiata* by *Dothistroma pini*. *New Zealand Journal of Forestry Science*, 4, 495-501. https://www.scionresearch.com/_data/assets/pdf_file/0007/58696/NZJFS431974GADGIL495_501.pdf

Gadgil, P.D. (1977). Duration of leaf wetness periods and infection of *Pinus radiata* by *Dothistroma pini*. *New Zealand Journal of Forestry Science*, 7, 83-90. https://www.scionresearch.com/_data/assets/pdf_file/0009/58977/NZJFS711977GADGIL83-90.pdf

Ganley, R.J., Williams, N.M., Rolando, C.A., Hood, I.A., Dungey, H.S., Beets, P.N., & Bulman, L.S. (2014). Management of red needle cast, caused by *Phytophthora pluvialis*, a new disease of radiata pine in New Zealand. *New Zealand Plant Protection*, 67, 48-53. <https://doi.org/10.30843/nzpp.2014.67.5721>

Garbelotto, M., & Hayden K.J. (2012). Sudden oak death: interactions of the exotic oomycete *Phytophthora ramorum* with naïve North American hosts. *Eukaryotic Cell*, 11(11). <https://doi.org/10.1128/ec.00195-12>

Gardner, J.F., Dick, M.A., & Bader, M.K.-F. (2015). Susceptibility of New Zealand flora to *Phytophthora kernoviae* and its seasonal variability in the field. *New Zealand Journal of Forestry Science*, 45: 23. <https://doi.org/10.1186/s40490-015-0050-y>

Gilmour, J.W. (1981). The effect of season on infection of *Pinus radiata* by *Dothistroma pini*. *European Journal of Forest Pathology*, 11, 265-269. <https://doi.org/10.1111/j.1439-0329.1981.tb00095.x>

Gilmour, J.W., & Noorderhaven, A. (1971). Influence of time of application of cuprous oxide on control of *Dothistroma* needle blight. *New Zealand Journal of Forestry Science*, 1, 160-166. https://www.scionresearch.com/_data/assets/pdf_file/0003/58611/NZJFS12GILMOUR160_166.pdf

Gilmour, J.W., Leggat, G.J., & Fitzpatrick, J. (1973). Operational control of *Dothistroma* needle blight in radiata pine plantations in New Zealand 1966-73. In *Proceedings of the 26th New Zealand weed and pest control conference* (pp. 130-138). <https://doi.org/10.30843/nzpp.1973.26.8936>

Gómez-Gallego, M., LeBoldus, J.M., Bader, M.K.-F., Hansen E., Donaldson, L., & Williams, N.M. (2019). Contrasting the pathogen loads in co-existing populations of *Phytophthora pluvialis* and *Nothophaeocryptopus gaeumannii* in Douglas fir plantations in New Zealand and the Pacific Northwest United States. *Phytopathology*, 109, 1908-1921. <https://doi.org/10.1094/PHYTO-12-18-0479-R>

Hansen, E.M., Reeser, P., Sutton, W., Gardner, J., & Williams, N. (2015). First report of *Phytophthora pluvialis* causing needle loss and shoot dieback on Douglas-fir in Oregon and New Zealand. *Plant Disease* 99(5), 727. <https://doi.org/10.1094/PDIS-09-14-0943-PDN>

Harrison J.G. (1992). Effects of the aerial environment on late blight of potato - a review. *Plant Pathology*, 41, 384-416. <https://doi.org/10.1111/j.1365-3059.1992.tb02435.x>

Hood, I.A., Williams, N.M., & Rolando, C.A. (2017). Towards a treatment regime for red needle cast. *Forest Health News*, 273, 1-2. Rotorua, New Zealand: Scion. <https://cdm20044.contentdm.oclc.org/digital/collection/p20044coll2/id/198/rec/1>

Hood, I.A., Husheer, S., Gardner, J.F., Evanson, T.W., Tieman, G., Banham, C., Wright, L.A.H., & Fraser, S. (2022). Infection periods of *Phytophthora pluvialis* and *Phytophthora kernoviae* in relation to weather variables and season in *Pinus radiata* forests in New Zealand. *New Zealand Journal of Forestry Science*, 52, 17. <https://doi.org/10.33494/nzjfs522022x224x>

Kuhn, M., Vaughan, D., & Hvitfeldt, E. (2024a). *yardstick*: Tidy characterizations of model performance. [R package version 1.3.1]. <https://CRAN.R-project.org/package=yardstick>. Accessed 12 March 2025.

Kuhn, M., Vaughan, D., & Hvitfeldt, E. (2024b). *parsnip*: A common API to modeling and analysis functions. [R package version 1.2.1]. <https://CRAN.R-project.org/package=parsnip>. Accessed 12 March 2025.

Lee E.H., Beedlow, P.A., Waschmann, R.S., Burdick, C.A., & Shaw, D.C (2013). Tree-ring analysis of the fungal disease Swiss needle cast in western Oregon coastal forests. *Canadian Journal of Forest Research*, 43, 677-690. <https://doi.org/10.1139/cjfr-2013-0062>

Manzano, J.M.M., Molina, R.T., Rodríguez, S.F., Barroso, P.D., Palacios, I.S., & Garijo, Á.G. (2015). Airborne propagules of *Phytophthora* and related taxa in SW Spain including a predictive model. *European Journal of Plant Pathology*, 143, 473-483. <https://doi.org/10.1007/s10658-015-0700-1>

McDougal, R., Cunningham, L., Hunter, S., Caird, A., Flint, H., Lewis, A., & Ganley, R. (2021). Molecular detection of *Phytophthora pluvialis*, the causal agent of red needle cast in *Pinus radiata*. *Journal of Microbiological Methods*, 189, 106299. <https://doi.org/10.1016/j.mimet.2021.106299>

McLay, E., Rogan, B., & Dobbie, K. (2023). First report of *Phytophthora pluvialis* causing needle lesions on *Pinus pinea* in New Zealand. *New Disease Reports*, 47(1): e12150. <https://doi.org/10.1002/ndr2.12150>

McLay, E., Lane, D., Turner, R.M., Somchit, C., Small, C., Banham, C., & Fraser, S. (2025). Impact of temperature on infection and sporulation of *Phytophthora pluvialis* on *Pinus radiata*. *Plant*

Pathology, 74(6) 1681-1696. <https://doi.org/10.1111/ppa.14116>

Migliorini, D., Ghelardini, L., Luchi, N., Capretti, P., Onorari, M., & Santini, A. (2019). Temporal patterns of airborne *Phytophthora* spp. in a woody plant nursery area detected using real-time PCR. *Aerobiologia*, 35, 201-214. <https://doi.org/10.1007/s10453-018-09551-1>

Milborrow S. (2024). *rpart.plot: Plot 'rpart' Models: An enhanced version of 'plot.rpart'*. [R package version 3.1.2] <https://CRAN.R-project.org/package=rpart.plot>. Accessed 12 March 2025.

O'Neill, R., McDougal, R., Fraser, S., Banham, C., Cook, M., Claasen, A., Simpson, S., & Williams, N. (2018). Validating outsourced high throughput automated qPCR for increased research outputs from forest pathology trials. *New Zealand Plant Protection*, 71, 355. <https://doi.org/10.30843/nzpp.2018.71.207>

O'Neill, R., McLay, E., Nunes Leite, L., Panda, P., Pérez-Sierra, A., Eacock, A., Le Boldus, J.M., Stamm, E.A., Fraser, S., & McDougal, R.L. (2025). Ultra-sensitive detection of *Phytophthora pluvialis* by real-time PCR targeting a mitochondrial gene. *bioRxiv* 2024.12.18.629255; <https://doi.org/10.1101/2024.12.18.629255>

Parker, A.K. (1972). Artificial inoculation of *Pinus radiata* with *Scirrhia (Dothistroma) pini*: effect of relative humidity and temperature on incubation. *Phytopathology*, 62, 1160-1164. <https://doi.org/10.1094/Phyto-62-1160>

Pearse, G.D., Jayathunga, S., Camarretta, N., Palmer, M.E., Steer, B.S.C., Watt, M.S., Watt, P., & Holdaway, A. (2025). Developing a forest description from remote sensing: Insights from New Zealand. *Science of Remote Sensing*, 11, 100183. <https://doi.org/10.1016/j.srs.2024.100183>

Pérez-Sierra, A., Chitty, R., Eacock, A., Jones, B., Biddle, M., Crampton, M., Lewis, A., Olivieri, L., & Webber, J.F. (2022). First report of *Phytophthora pluvialis* in Europe causing resinous cankers on western hemlock. *New Disease Reports*, 45: e12064. <https://doi.org/10.1002/ndr2.12064>

Pérez-Sierra, A., Chitty, R., Eacock, A., Wylder, B., Biddle, M., Quick, C., Gorton, C., Olivieri, L., & Crampton, M. (2024). First report of *Phytophthora pluvialis* causing cankers on Japanese larch in the United Kingdom. *New Disease Reports*, 49: e12246. <https://doi.org/10.1002/ndr2.12246>

Peterson, G.W. (1973). Infection of Austrian and ponderosa pines by *Dothistroma pini* in eastern Nebraska. *Phytopathology*, 63, 1060-1063. <https://doi.org/10.1094/Phyto-63-1060>

Peterson, E.K., Hansen, E.M., & Kanaskie, A. (2015). Temporal epidemiology of sudden oak death in Oregon. *Phytopathology*, 105, 937-946. <https://doi.org/10.1094/PHYTO-12-14-0348-FI>

Pirronitto, S., Paquet, F., Gaucet, V., & Chandelier, A. (2024). First report of *Phytophthora pluvialis* in Douglas fir plantations in Belgium. *New Disease Reports*, 49(1): e12244. <https://doi.org/10.1002/ndr2.12244>

R Core Team (2022). *R: A language and environment for statistical computing*. Vienna, Austria: R Foundation for Statistical Computing. <https://www.r-project.org/>. Accessed 12 March 2025.

Reeser, P., Sutton, W., & Hansen, E. (2013). *Phytophthora pluvialis*, a new species from mixed tanoak-Douglas-fir forests of western Oregon, U.S.A. *North American Fungi*, 8(7), 1-8. https://www.fs.usda.gov/psw/publications/sod/psw_2013_sod004_reeser.pdf

Schena, L., Hughes, K.J.D., & Cooke, D.E.L. (2006). Detection and quantification of *Phytophthora ramorum*, *P. kernoviae*, *P. citricola* and *P. quercina* in symptomatic leaves by multiplex real-time PCR. *Molecular Plant Pathology*, 7(5), 365-379. <https://doi.org/10.1111/j.1364-3703.2006.00345.x>

Tabima, J.F., Gonen, L., Gómez-Gallego, M., Panda, P., Grünwald, N.J., Hansen, E.M., McDougal, R., LeBoldus, J.M., & Williams, N.M. (2021). Molecular phylogenomics and population structure of *Phytophthora pluvialis*. *Phytopathology*, 111(1), 108-115. <https://doi.org/10.1094/PHYTO-06-20-0232-FI>

Taylor, M.C., Hardwick, N.V., Bradshaw, N.J., & Hall, M.A. (2003). Relative performance of five forecasting schemes for potato late blight (*Phytophthora infestans*) I. Accuracy of infection warnings and reduction of unnecessary, theoretical, fungicide applications. *Crop Protection*, 22, 275-283. [https://doi.org/10.1016/S0261-2194\(02\)00148-5](https://doi.org/10.1016/S0261-2194(02)00148-5)

Therneau T., Atkinson B., & Ripley, B. (2022). *rpart: Recursive partitioning and regression trees*. [R package version 4.1.19] <https://CRAN.R-project.org/package=rpart>. Accessed 12 March 2025.

Van der Plank, J.E. (1963). *Plant diseases: epidemics and control*, 349 pp. Academic Press, New York.

Watt, M.S., Palmer, D.J., & Bulman, L.S. (2011). Predicting the severity of Dothistroma on *Pinus radiata* under current climate in New Zealand. *Forest Ecology and Management*, 261(11), 1792-1798. <https://doi.org/10.1016/j.foreco.2011.01.043>

Watt, M.S., Holdaway, A., Watt, P., Pearse, G.D., Palmer, M.E., Steer, B.S.C., Camarretta, N., McLay, E. & Fraser, S. (2024). Early prediction of regional red needle cast outbreaks using climatic data trends and satellite-derived observations. *Remote Sensing*, 16(8): 1401. <https://doi.org/10.3390/rs16081401>

Wickham H., Averick M., Bryan J., Chang W., McGowan L.D., François R., Grolemund G., Hayes A., Henry L., Hester J., Kuhn M., Pedersen T.L., Miller E., Bache S.M., Müller K., Ooms J., Robinson D., Seidel D.P., Spinu V., Takahashi K., Vaughan D., Wilke C., Woo K., & Yutani H. (2019). Welcome to the tidyverse. *Journal of Open Source Software*, 4(43): 1686. <https://doi.org/10.21105/joss.01686>

Woods, A., Coates, K.D., & Hamann, A. (2005). Is an unprecedented Dothistroma needle blight epidemic related to climate change? *Bioscience*, 55(9), 761-769. [https://doi.org/10.1641/0006-3568\(2005\)055\[0761:IAUDNB\]2.0.CO;2](https://doi.org/10.1641/0006-3568(2005)055[0761:IAUDNB]2.0.CO;2)

Woods, A.J., Martín-García, J., Bulman, L., Vasconcelos, M.W., Boberg, J., La Porta, N., Peredo, H., Vergara, G., Ahumada, R., Brown, A., & Diez, J.J. (2016). Dothistroma needle blight, weather and possible climatic triggers for the disease's recent emergence. *Forest Pathology*, 46, 443-452. <https://doi.org/10.1111/efp.12248>

SUPPLEMENTARY TABLES

TABLE S1: Sites assessed in 2024. Analysis of red needle cast data from 2024 was not undertaken due to the small number of remaining sites^a.

| Site | % of trees with RNC | % RNC on worst tree | RNC index (%) |
|------|---------------------|---------------------|---------------|
| 6 | 0 | 0 | 0 |
| 10 | 0 | 0 | 0 |
| 12 | 0 | 0 | 0 |
| 16 | 0 | 0 | 0 |
| 17 | 35 | 20 | 7 |
| 27 | 95 | 40 | 38 |
| 32 | 0 | 0 | 0 |
| 33 | 0 | 0 | 0 |
| 35 | 0 | 0 | 0 |
| 35b | 0 | 0 | 0 |
| 36 | 0 | 0 | 0 |
| 37 | 0 | 0 | 0 |
| 38 | 0 | 0 | 0 |
| 40 | 0 | 0 | 0 |
| 42 | 0 | 0 | 0 |
| 43 | 0 | 0 | 0 |
| 44 | 0 | 0 | 0 |
| 45 | 5 | 35 | 2 |
| 51 | 25 | 90 | 23 |

^aSites 6-38, Central North Island (mean index, 3.5 %); Sites 40-51, Gisborne Region (mean index, 4.2 %).

TABLE S2: Details of known cuprous oxide application to study sites. Red needle cast data for years following application were removed from analysis (rows coloured red).

| Site | Year | Disease index (%) | Spray history | <i>P. pluvialis</i> detection |
|------|------|-------------------|---------------------|-------------------------------|
| 10 | 2014 | NA | Dec 2014 & Feb 2015 | |
| | 2015 | 4 | | |
| | 2016 | 35 | | Immuno Strip |
| | 2017 | 14 | | |
| | 2018 | 0 | | |
| | 2019 | 0 | | |
| | 2020 | 0 | | |
| | 2021 | 0 | | |
| | 2022 | 27 | | |
| | 2023 | 12 | | |
| 31 | 2014 | NA | | |
| | 2015 | 1 | | |
| | 2016 | 30 | Nov | Immuno Strip |
| | 2017 | 64 | | |
| | 2018 | 8 | Dec | |
| | 2019 | 0 | | |
| | 2020 | 0 | | |
| | 2021 | 0 | | |
| | 2022 | 0 | | |
| | 2023 | NA | | qPCR |

TABLE S2: *continued*

| Site | Year | Disease index (%) | Spray history | <i>P. pluvialis</i> detection |
|------|------|-------------------|---------------------|-------------------------------|
| 32 | 2014 | NA | | |
| | 2015 | 29 | | Culture |
| | 2016 | 27 | | |
| | 2017 | 45 | | |
| | 2018 | 2 | Oct 2018 & Feb 2019 | |
| | 2019 | 0 | | |
| | 2020 | 1 | | |
| | 2021 | 35 | | qPCR |
| | 2022 | 3 | | qPCR & Culture |
| | 2023 | 30 | | |
| 34 | 2014 | NA | | |
| | 2015 | 5 | | Culture |
| | 2016 | 28 | Oct | |
| | 2017 | 60 | | |
| | 2018 | 0 | Oct | |
| | 2019 | 1 | | qPCR |
| | 2020 | 0 | | |
| | 2021 | 7 | | qPCR & Culture |
| | 2022 | 1 | | |
| | 2023 | NA | | |
| 35b | 2014 | NA | Nov | |
| | 2015 | 27 | | |
| | 2016 | 62 | Oct | |
| | 2017 | 0 | | |
| | 2018 | 0 | | |
| | 2019 | 0 | | |
| | 2020 | 1 | | |
| | 2021 | 4 | | |
| | 2022 | 15 | | qPCR & Culture |
| | 2023 | 72 | | |
| 36 | 2014 | NA | | |
| | 2015 | 19 | | |
| | 2016 | 59 | Oct | |
| | 2017 | 0 | | |
| | 2018 | 32 | | qPCR & Culture |
| | 2019 | 0 | Nov | |
| | 2020 | 0 | | |
| | 2021 | 0 | | |
| | 2022 | 54 | | |
| | 2023 | 80 | | |
| 37 | 2014 | NA | | |
| | 2015 | 16 | Nov 2015 & Feb 2016 | |
| | 2016 | 14 | | |
| | 2017 | 0 | | |
| | 2018 | 1 | | |
| | 2019 | 0 | | |
| | 2020 | 0 | | |
| | 2021 | 0 | | |
| | 2022 | 0 | | qPCR & Culture |
| | 2023 | 80 | | qPCR |

TABLE S3: Details of *Phytophthora pluvialis* cultures from this study held in Scion's National Forest Culture Collection

| Site ID | Year collected | NZFS Number(s) |
|---------|----------------|--------------------|
| 6 | 2022 | NZFS5503 |
| 30 | 2022 | NZFS5501 |
| 32 | 2015 | NZFS4171, NZFS4173 |
| 33 | 2015 | NZFS4268 |
| 34 | 2015 | NZFS4172 |
| 34 | 2021 | NZFS5389 |
| 35 | 2022 | NZFS5502 |
| 36 | 2018 | NZFS5181 |
| 40 | 2018 | NZFS5182, NZFS5183 |
| 41 | 2018 | NZFS5184 |
| 42 | 2020 | NZFS5266 |
| 43 | 2018 | NZFS5185 |
| 45 | 2018 | NZFS5186, NZFS5187 |
| 48 | 2018 | NZFS5188, NZFS5189 |
| 49 | 2018 | NZFS5190 |
| 49 | 2020 | NZFS5263 |
| 50 | 2018 | NZFS5191, NZFS5192 |
| 50 | 2020 | NZFS5267 |
| 51 | 2018 | NZFS5193, NZFS5194 |